

Chapter 5

The Imprint of Species Turnover on Old-Growth Forest Carbon Balances – Insights From a Trait-Based Model of Forest Dynamics

Christian Wirth and Jeremy W. Lichstein

5.1 Introduction

Succession is the process that eventually transforms a young forest into an old-growth forest. Describing and analysing plant succession has been at the core of ecology since its early days some hundred years ago. With respect to forest succession, our understanding has progressed from descriptive classifications (i.e. identifying which forest types constitute a successional sequence) to general theories of forest succession (Watt 1947; Horn 1974, 1981; Botkin 1981; West et al. 1981; Shugart 1984) and simulation models of forest dynamics that are capable of predicting successional pathways with remarkable precision (Urban et al. 1991; Pacala et al. 1996; Shugart and Smith 1996; Badeck et al. 2001; Bugmann 2001; Hickler et al. 2004; Purves et al. 2008).

Although the importance of different factors in controlling successional changes in species composition is still debated – particularly in speciose tropical forests (Hubbell 2001) – a large body of evidence implicates the tradeoff between shade-tolerance and high-light growth rate as a key driver (Bazzaz 1979; Pacala et al. 1994; Wright et al. 2003). In contrast, there is no well-accepted mechanism to explain successional changes in forest biomass, much less other components of ecosystem carbon. A range of biomass trajectories have been observed (e.g. monotonic vs hump-shaped curves), and some basic ideas have been proposed to explain these patterns (Peet 1981, 1992; Shugart 1984). However, we are aware of only one systematic, geographically extensive assessment of biomass trajectories (see Chap. 14 by Lichstein et al., this volume). In this data vacuum, it has been difficult to assess the relative merits of different theories or mechanisms. This is especially true for later stages of forest succession, and in particular for old-growth forests.

With respect to biomass dynamics, there are at least four non-mutually exclusive hypotheses: (1) the ‘equilibrium hypothesis’ of Odum (1969); (2) the ‘stand-breakup hypothesis’ of Bormann and Likens (1979) and its generalisations (e.g. Peet 1981, 1992; Shugart 1984); (3) the hypothesis of Shugart and West (1981), which we term the ‘shifting-traits hypothesis’; and (4) the ‘continuous accumulation hypothesis’ of Schulze et al. (Chap. 15, this volume). Because some of these

hypotheses are discussed in greater detail in later chapters of this book (e.g. Lichstein et al., Chap. 14), we will only briefly summarise their main features here.

The equilibrium hypothesis of Odum (1969) states that, as succession proceeds, forests approach an equilibrium biomass where constant net primary production (NPP) is balanced by constant mortality losses. These losses are passed on to the woody detritus compartment, which will itself equilibrate when mortality inputs are balanced by heterotrophic respiration and carbon transfers to the soil. This logic may be extended to soil carbon pools, but the validity of the equilibrium hypothesis for soil carbon is challenged by Reichstein et al. (Chap. 12, this volume); this is therefore not addressed in the present chapter. Odum makes no strict statements about how ecosystems actually approach the assumed equilibrium, but views a monotonic increase to an asymptote as typical. In addition, it follows from Odum's hypothesis that, once equilibrium is reached, an 'age-related decline' in NPP would induce a biomass decline given a constant mortality (see Chap. 21 by Wirth, this volume).

The 'stand-breakup hypothesis' assumes synchronised mortality of canopy trees after stands have reached maturity. As the canopy breaks up, the stand undergoes a transition from an even-aged mature stand of peak biomass to a stand comprised of a mixture of different aged patches and, therefore, lower mean biomass (Watt 1947; Bormann and Likens 1979). Peet (1981) generalised this hypothesis by allowing for lagged regeneration (formalised in Shugart 1984), which may result in biomass oscillations. In any case, the mortality pulse at the time of canopy break-up would result not only in declining biomass, but also in an increase in woody detritus.

The 'shifting traits hypothesis' states that biomass and woody detritus trajectories reflect successional changes in species traits, which follow from successional changes in species composition. Relevant traits, which are also typically used in gap models of forest succession, include maximum height, maximum longevity, wood density, shade tolerance, and decay-rate constants of woody detritus (Doyle 1981; Franklin and Hemstrom 1981; Shugart and West 1981; Paré and Bergeron 1995). The reasoning is straightforward: The maximum height defines the upper boundary of the total aboveground ecosystem volume that can be filled with stem volume. Shade tolerance and wood density modulate the degree to which this volume can be filled with biomass. The combination of these three parameters thus determines the maximum size of the aboveground carbon pool for a given species. Tree longevity controls how long a species' pool remains filled with biomass carbon. Similarly, wood decay-rate affects the dynamics of the woody detritus carbon pool.

Finally, the 'continuous accumulation hypothesis' of Schulze et al. (Chap. 15, this volume) states that, by and large, natural disturbance cycles in temperate and boreal systems are too short for us to make generalisations about the long-term fate of aboveground carbon pools, and that during the comparatively narrow observational time-window, accumulation is the dominant process.

It is one of the goals of this book to review empirical evidence for carbon trajectories predicted by these different hypotheses. Successional trajectories of aboveground carbon stocks can, in principle, be derived from large-scale forest inventories (see Chaps. 14 and 15 by Lichstein et al. and Schulze et al., respectively;

Wirth et al. 2004b). However, in those countries where extensive and well-designed inventories are available, little old forest remains; and even large inventories do not provide a comprehensive picture of old-growth carbon trajectories (see Chap. 14 by Lichstein et al., this volume). Alternatively, long-term chronosequences could be used. As we discuss below (see Sect. 5.7), the number of chronosequences extending into the old-growth phase is limited and by no means representative. It appears that the empirical evidence for old-growth carbon trajectories is insufficient to differentiate between the extant hypotheses and to assess their relevance for natural landscapes.

In this chapter, we present a model that was designed to assess the potential contribution of the ‘shifting-traits’ mechanism to forest carbon dynamics. The model was tailored to work with two unusually rich sources of information: the abundant trait data available for nearly all United States (US) tree species, and detailed descriptions of successional species turnover in different US forest types. The work presented in this chapter constitutes, to our knowledge, the first systematic evaluation of the ‘shifting traits hypothesis’.

Specifically, the model uses four widely available tree traits (maximum height, longevity, wood density, and woody decay rates) to translate qualitative descriptions of succession for a vast number of forest types into quantitative predictions of aboveground carbon stock trajectories. We focused on US forests because only here could we find sufficient information for both model parameterisation and validation (see Chap. 14 by Lichstein et al., this volume). We first describe the model parameterisation and simulations. Next, we characterise how the input trait data for the 182 tree species relate to successional status. After validating the model with data from the old-growth literature, we use the model to calculate aboveground carbon trajectories, including woody detritus, for 106 North American forest types. The results provide insights into the factors controlling the shapes of forest carbon trajectories and the capacity of the biomass and deadwood pools to act as carbon sinks in old-growth forests.

5.2 A Trait-Based Model of Forest Carbon Dynamics

5.2.1 *Successional Guilds*

One of the most obvious features of forest succession is a gradual change in species composition. The dominant tree species in old-growth stands are not likely to be the species that dominated when the community was founded a few hundred years before. Depending on when species tend to dominate in the course of succession, we refer to them as early-, mid- or late-successional. The mechanism by which these three guilds replace each other may vary (West et al. 1981; Glenn-Lewin et al. 1992). The model developed in this chapter does not attempt to capture the mechanisms leading to species turnover, but rather takes this

turnover as given and prescribes it according to empirical descriptions (see below). Therefore, we mention the mechanisms of species turnover only briefly here.

Most commonly, it is assumed that species turn over via gap-phase dynamics; i.e. succeeding species arrive and grow in canopy gaps created by the death of individuals of earlier successional species. Alternatively, all species may arrive simultaneously, and differences in longevity or maximum size may allow the successor species to either outlive or outgrow the initially dominant species (see Fig. 15.8 in Schulze et al., Chap. 15, for an example).

The three guilds differ in many ways but most prominently with respect to their tolerance of shading. Forest scientists have grouped tree species according to shade tolerance (Niinemets and Valladares 2006). Usually, an ordinal scale with five levels is employed, ranging from 1 (very intolerant) to 5 (very tolerant), and these classes are often used to infer a species' successional niche. The physiological and demographic underpinnings of shade tolerance have been intensively studied (see Chaps. 4 and 6 by Kutsch et al. and Messier et al., respectively), and there is a long list of associated physiological and morphological traits (Kobe et al. 1995; Lusk and Contreras 1999; Walters and Reich 1999; Henry and Aarssen 2001; Körner 2005). In this chapter we apply the concept of shade tolerance to sort species into early-, mid- and late-successional species.

5.2.2 Model Structure

We first describe the model structure. The data used to parameterise the model are described in Sect. 5.2.3. We simulated a stochastic patch model with an annual time-step. Each patch is 10×10 m and contains a single monospecific cohort that grows in height and simultaneously accumulates biomass. Thus, the model simulates the dynamics of volume and biomass of cohorts, not individuals. Each patch experiences stochastic whole-patch mortality (see below), after which a new cohort of height zero is initiated. At the beginning of the simulation, each patch is initialised with the pioneer species of a given successional sequence (see Sect. 5.2.3), which, upon whole-patch mortality, are replaced by mid-successional species, which in turn are replaced by late-successional species. From then on, late-successional species replace themselves. We simulated the dynamics of 900 independent patches for each forest type and report the ensemble means of the bio- and necromass-dynamics.

In each patch i , the cohort increases in height H (m) according to a Michaelis-Menten-type curve:

$$H_i(t') = \frac{h_{\max} t'}{(h_{\max}/h_s) + t'} \quad 5.1$$

where t' (years) denotes the time since cohort initiation, h_{\max} the asymptotic height, and h_s the initial slope of the height-age curve of a given species. Cohort height is converted to stand volume V ($\text{m}^3 \text{m}^{-2}$) as

$$V(t') = \underbrace{(\beta_0 + \beta_1 \tau)}_{\beta_0^*} H(t')^{\beta_2} \quad 5.2$$

where the coefficient β_0^* depends on a species' shade-tolerance τ (from 1 = very intolerant to 5 = very tolerant). Values of β were estimated separately for conifers and hardwoods using European yield tables (Wimmenauer 1919; Tjurin and Naumenko 1956; McArdle 1961; Assmann and Franz 1965; Wenk et al. 1985; Dittmar et al. 1986; Erteld et al. 1962). These yield tables were constructed from long-term permanent sample plots and thinning trials and provide data on canopy height (mean height of dominant trees) and merchantable wood volume for a range of site conditions for a total of 21 European and North American species. Because the yield tables represent monospecific, even-aged stands, Eq. 5.2 does not include sub-canopy cohorts. For both taxonomic groups, the values of β_1 were positive; i.e. for a given canopy height, stands of shade-tolerant tree species contain more stem volume than stands of light-demanding tree species. This probably reflects the fact that shade-tolerant species are better able to survive under crowded conditions.

Volume is converted to biomass carbon C_b (kg m^{-2}) as

$$C_b(t', H) = V(t') \cdot \rho \cdot c \cdot \theta \cdot e(H) \quad 5.3$$

Here, ρ is the species-specific wood density, and c is the carbon concentration of biomass (Table 5.1). The tuning parameter θ corrects for several biases in our model and/or parameterisation: (1) the yield-table parameterisation (see above) ignores sub-canopy trees present in natural forests; (2) advanced regeneration may survive canopy mortality events, so that patch height may not, in reality, start at a height of 0 as assumed in our model; and (3) stand densities in forest trials used to construct the yield tables tend to be lower than in natural forests. The value of θ was adjusted to maximise the overall fit to the validation dataset (Sect. 5.4). Because θ was set constant across all species, it corrects for overall bias of modelled carbon stocks but does not influence the shapes of the carbon-stock trajectories over time. Finally, the crown biomass expansion factor e (the ratio of total aboveground biomass to stem biomass) decreases with patch height as

$$e(H) = \varepsilon_1 + (\varepsilon_2 - \varepsilon_1) \cdot \exp(-\varepsilon_3 H) \quad 5.4$$

where ε_1 and ε_2 are the minimum and maximum expansion factors, respectively, and ε_3 controls the rate of decline in e with patch height. We used the parameters ε_1 and ε_2 for conifers and hardwoods given in Wirth et al. (2004a).

We distinguish two types of mortality resulting in woody-detritus production: self-thinning and whole-patch mortality. Self-thinning is represented as a carbon

Table 5.1 Model parameters, values (C conifers; H hardwood) and units

Parameter	Meaning	Value	Unit
h_{\max}	Maximum height	Species-specific	m
h_s	Initial slope of height–age curve	0.6	m year^{-1}
β_0	Baseline coefficient of height–stem volume allometry	C: 2.14, H:1.26	$\text{m}^3 \text{ha}^{-1}$
β_1	Control of shade–tolerance over β_0	C: 0.53, H: 0.15	$\text{m}^3 \text{ha}^{-1}$
β_2	Exponent of H-volume allometry	C: 1.47, H: 1.59	$\text{m}^3 \text{ha}^{-1}$
c	Carbon concentration of biomass	0.5	$\text{kg C kg}^{-1} \text{dw}^b$
ρ	Wood density	Species-specific	$\text{kg}_{\text{dw}} \text{m}^{-3} \text{fv}^c$
θ	Tuning parameter	2	Unitless
ε_1	Maximum ABEF ^a at zero height	C: 5.54, H: 1.71	kg kg^{-1}
ε_2	Shape factor for ABEF decline	C: 0.22, H: 1.80	Unitless
ε_3	Lower positive asymptote of ABEF	C: 1.31, H: 1.27	kg kg^{-1}
λ	Longevity	Species-specific	year
k_d	Woody detritus decay constant	C: 0.03, H: 0.10	year^{-1}
δ_1	Fraction of h_{\max} where μ equals 0.5	0.5	Unitless
δ_2	Fraction of h_{\max} where μ equals f	0.75	Unitless
f	Fraction of μ^* at $0.75 h_{\max}$	0.95	Unitless

^aAboveground biomass expansion factors

^bdw = dry weight

^cfv = fresh volume

flux to the woody detritus pool that is set proportional to biomass accumulation. Specifically, in accordance with data from forest trials with low thinning intensity, the rate of woody-detritus production resulting from self-thinning was assumed to be one-half that of biomass accumulation (Assmann 1961). This implies that, in mature stands with little net biomass accumulation (which approaches zero in our model as patch height approaches h_{\max} , see Eqs. 5.1 and 5.2), self-thinning is minimal and woody detritus production results primarily from whole-patch mortality. Although this scheme ignores branch-fall in mature stands, it provides a reasonable approximation to reality. Unlike self-thinning, whole-patch mortality (which resets cohort height, and thus aboveground biomass, to zero) is stochastic and occurs at each annual time-step (in each patch independently) with probability μ . We assume that μ can be approximated by the individual-tree mortality rate μ^* , which we estimate from maximum tree longevity λ , as is commonly done in gap models (Shugart 1984). Longevity can be viewed as the time span after which the population has been reduced to a small fraction $\phi \equiv (1 - \mu^*)^\lambda$, where we set $\phi = 0.01$; i.e. we assume that 1% of individuals survive to age λ . The annual individual mortality rate is thus $\mu^* = 1 - \sqrt[\lambda]{0.01}$. Note that we are applying this per-capita rate to a whole patch of 10×10 m. Therefore, it shall become effective only for patches that are occupied by a single large tree. To accomplish this, we assume that μ is size dependent, such that it is near zero in young patches (where most mortality occurs due to self thinning), and increases asymptotically to μ^* as

patch height approaches h_{\max} . Specifically, we assume that μ is equal to the product of μ^* and a patch-height-dependent logistic function (Fig. 5.1):

$$\mu = \mu^* \cdot \frac{e^{\vartheta(H)}}{1 + e^{\vartheta(H)}} \quad 5.5$$

where

$$\vartheta(H) = \frac{\ln(f/(1-f))}{h_{\max}(\delta_2 - \delta_1)} (H - \delta_1 h_{\max}) \quad 5.6$$

According to Eq. 5.5, μ is $0.5\mu^*$ when H is $\delta_1 h_{\max}$, and μ is $f\mu^*$ when H is $\delta_2 h_{\max}$. We assigned δ_1 , δ_2 , and f the values 0.5, 0.75, and 0.95, respectively. This parameterisation yields a monotonically increasing approach to μ^* , with $\mu = 0.5\mu^*$ when $H = 0.5h_{\max}$, and $\mu = 0.95\mu^*$ when $H = 0.75h_{\max}$ (Fig. 5.1). In our simulations, these parameter values yield a smooth upward transition (no hump-shaped trajectory) to an equilibrium biomass, although other values result in a biomass peak followed by oscillations (results not shown). This complex behaviour (which was avoided in the simulations presented in this chapter) results from synchronised mortality across patches when there is a sudden transition from $\mu \approx 0$ to $\mu \approx \mu^*$.

Finally, note that as μ increases to its asymptote, mortality due to self-thinning declines to zero (see above); thus, the total mortality rate in a patch is constrained to reasonable values at all times.

Both self-thinning and whole-patch mortality result in a transfer of biomass to the woody detritus pool C_d , creating input $I_d(t)$. Woody detritus input from branch shedding by live trees is not taken into account. Decay of woody detritus is modelled according to first-order kinetics (Olsen 1981). The change in woody detritus carbon stocks is modelled as a discrete time-step version of the differential equation

$$\frac{dC_d}{dt} = I_d(t) - k_d C_d(t) \quad 5.7$$

where k_d is the exponential annual decomposition rate constant.

5.2.3 Input Data

Trait data were assembled as part of the *Functional Ecology of Trees* (FET) database project (Kattge et al. 2008). To conserve space, we mention only the main data sources here. Maximum heights and longevity were obtained from Burns and Honkala (1990) and the *Fire Effects Information System* database (<http://www.fs.fed.us/database/feis/>). Shade tolerances were taken from Burns and

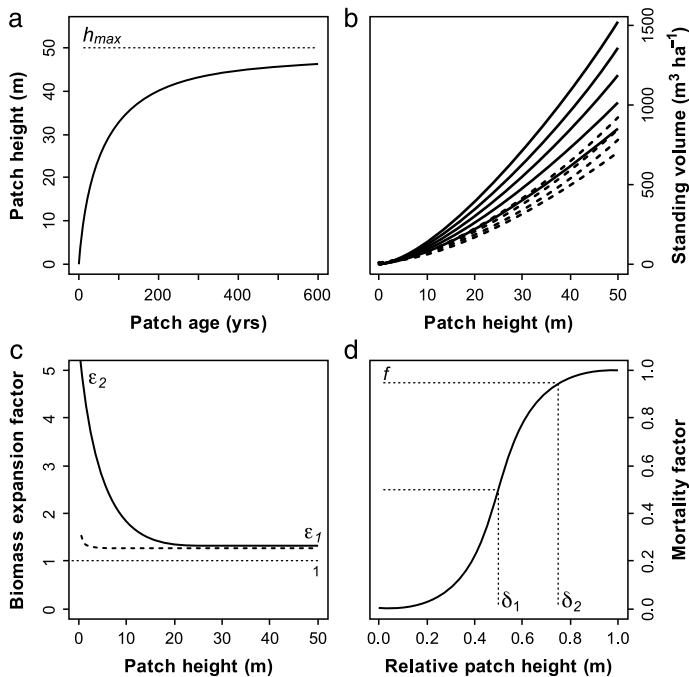


Fig.5.1a–d Illustration of main functions used in the model. **a** Height-age curve governed by the parameters maximum height h_{max} (dotted line) and initial slope h_s (Eq. 5.1). **b** Allometric relationship between patch height and stem volume (Eq. 5.2) for conifers (solid line) and hardwoods (dashed line) for different shade-tolerance classes (lowermost curves = very intolerant; uppermost curves = very tolerant), fitted from volume yield tables. **c** Relationship between the aboveground biomass expansion factor e and patch height for conifers (solid line) and hardwoods (dashed line) (Eq. 5.4). **d** Whole-patch mortality rate (proportion of asymptotic value) as a function of patch height (Eqs. 5.5, 5.6)

Honkala (1990) and Niinemets and Valladares (2006). The majority of wood density data were obtained from Jenkins et al. (2004). Decomposition rates of coarse woody detritus for conifers and hardwoods were derived from the FET database comprising over 500 observations of k_d from 74 tree species in temperate and boreal forest (C. Wirth, unpublished).

Species-specific parameters were assigned for maximum height h_{max} , maximum longevity λ , shade-tolerance τ , and basic wood density ρ . Due to data limitations, the following parameters were assigned at the level of angiosperms (hardwoods) vs gymnosperms (conifers): decomposition rates for woody detritus, the base-line allometric coefficients relating cohort height to cohort volume, and parameters controlling the size-dependency of the biomass expansion factors (see below). All other parameters were constants across all species (Table 5.1).

Successional sequences of species replacements were based on detailed descriptions of North American forest cover types (FCT) published by the Society of

American Foresters (Eyre 1980). Each FCT is described qualitatively in terms of its species composition, geographic distribution, site conditions, and dynamics. For each FCT, we noted which species were classified as dominant, co-dominant, or associated/admixed. We did not include species listed as ‘additional’, ‘occasional’, ‘rare’ or ‘subcanopy’. We then classified each species in each FCT as pioneer-, mid-, or late-successional. In many cases, these assignments were explicitly stated in the *ecological relationships* section of the description. Otherwise, we used shade-tolerances to assign species successional status as follows: pioneer ($\tau = 1$ or 2), mid-successional ($\tau = 3$), and late-successional ($\tau = 4$ or 5). Long-lived pioneer species ($\lambda > 400$ years) were assigned to all three successional guilds. Finally, for each FCT we calculated the weighted mean of the species-specific traits h_{\max} , λ , τ and ρ . Dominant species were given triple weight, co-dominant species double weight, and admixed species single weight. Conifer or hardwood trait values for k_d , ε_1 , ε_2 , and ε_3 , were used for successional stages dominated by either conifers or hardwoods. Mean values were used for mixed stages.

5.2.4 Model Setup

We simulated 2,000 years of succession for each of the 106 forest types. To isolate the importance of differences between conifers and hardwoods in woody detritus decay rates, we ran two sets of simulations, the first with $k_d = 0.05 \text{ year}^{-1}$ for both conifers and hardwoods, and the second with the standard parameterisation (Table 5.1), i.e. different k_d values for conifers and hardwoods. For each forest cover type, we report time-dependent means across the 900 patches for C_b , C_d , and their sum, C_a . In addition, we calculated aboveground net ecosystem productivity (ANEP) as the mean annual change in pool sizes, ΔC_x , for the following periods: (1) 0–100 years, (2) 101–200 years, (3) 201–400 years and (4) 401–600 years. We refer to these periods as ‘pioneer’, ‘transition’, ‘early old-growth’ and ‘late old-growth’ phases. Equilibrium biomasses in Fig. 5.4 were calculated as mean stocks from single-species runs between 1,000 and 2,000 years.

5.3 The Spectrum of Traits

Before we turn to the model predictions, we ask how the species-specific parameters influencing aboveground carbon stocks (h_{\max} , λ and ρ) vary with shade tolerance (‘intolerant’: $\tau = 1$ or 2; ‘intermediate’: $\tau = 3$; and ‘tolerant’: $\tau = 4$ or 5; Fig. 5.2). Recall that, in our model, these three shade-tolerance classes correspond to the pioneer, mid- and late-successional guilds, respectively.

Intolerant conifers and hardwoods reached similar maximum heights (means of 27 m and 31 m, respectively; Fig. 5.2a,b). As shade tolerance increased, conifers

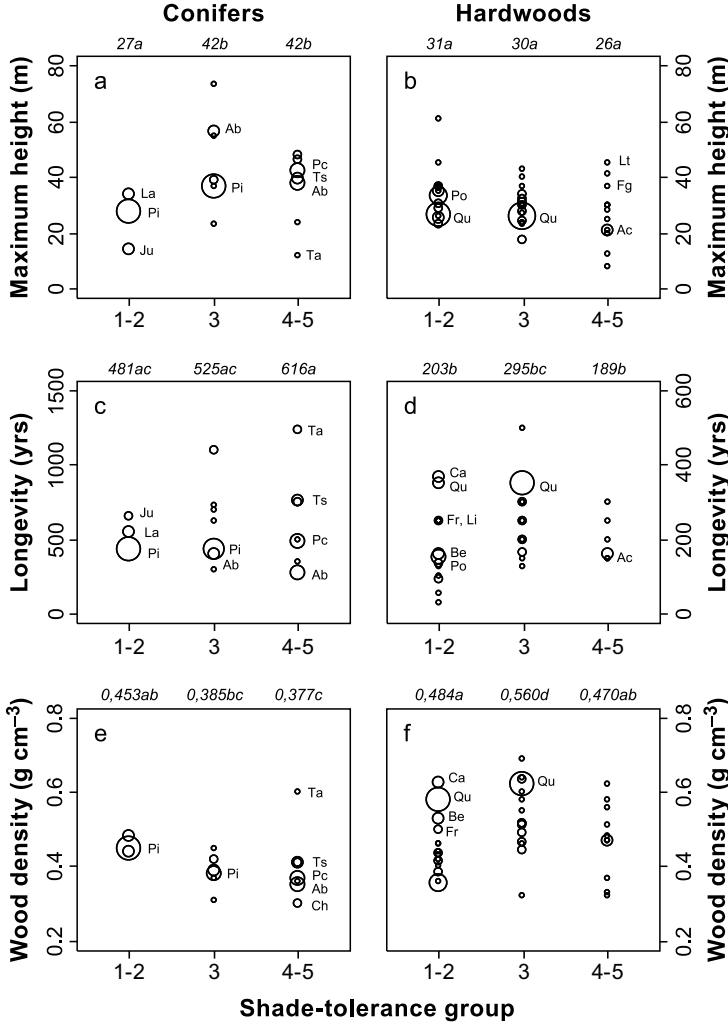


Fig. 5.2 Maximum height h_{\max} (a, b), maximum longevity λ (c, d) and wood density ρ (e, f) for coniferous and hardwood species (left and right panels, respectively) as a function of shade-tolerance class (1–2 intolerant, 3 intermediate, 4–5 tolerant) based on data for 182 North American tree species. Individual data points represent mean values for genera. The area of the circles is proportional to the number of species per genus. Figures at the top of the panel are means for each shade-tolerance class. The lower case letters indicate groups that are not significantly different (Tukey’s HSD post-hoc comparison including both conifers and hardwoods). Specific genera mentioned in the text are abbreviated as follows: Ab *Abies*, Ac *Acer*, Be *Betula*, Ca *Carya*, Ch *Chamaecyparis*, Fg *Fagus*, Fr *Fraxinus*, Ju *Juniperus*, La *Larix*, Lt *Lithocarpus*, Li *Liriodendron*, Pc *Picea*, Pi *Pinus*, Po *Populus*, Qu *Quercus*, Ta *Taxus*, Ts *Tsuga*, Tx *Taxodium*, Ul *Ulmus*

increased in h_{\max} to 42 m, but hardwoods decreased to 26 m. As a result, both intermediate and tolerant conifers were significantly taller by about 14 m than their hardwood counterparts. The high variance in h_{\max} in the tolerant groups is due to the existence of two functional groups: (1) relatively tall canopy species;

and (2) relatively short sub-canopy species, such *Acer pensylvanicum* and *Carpinus caroliniana* in the hardwoods, and *Taxus brevifolia* in the conifers. As mentioned above, sub-canopy trees were not included in the model simulations.

Tree longevity was not related to shade tolerance within either conifers or hardwoods but, for a given shade-tolerance class, conifers were about 300 years longer-lived than hardwoods (Fig. 5.2c,d). This difference between conifers and hardwoods was significant for the intolerant and tolerant classes. The intolerant hardwoods include two subgroups: short-lived species dominated by poplars (*Populus* spp.) and birches (*Betula* spp.) with longevities up to 150 years, and ‘long-lived pioneers’ (see Chap. 2 by Wirth et al., this volume), such as oaks (*Quercus* spp.) and hickories (*Carya* spp.), with longevities over 300 years. Nearly all intolerant conifers are long-lived, and most belong to the genus *Pinus*. Longevities of intolerant conifers range from 100 years (*Pinus clausa*) to 1,600 years (*Pinus aristata*) with a mean longevity of 480 ± 370 years (\pm standard deviation). The tolerant conifers are a particularly diverse group, with longevities ranging from 150 years (*Abies fraseri*) to 1,930 years (*Chamaecyparis nootkatensis*). True firs (*Abies* spp.), which tend to be shade tolerant, have among the lowest longevities of all conifers.

Wood density of conifers declined with increasing shade-tolerance, from about $0.45 \text{ g}_{\text{dw}} \text{ cm}^{-3}$ in intolerant genera (e.g. *Pinus*, *Larix* and *Juniperus*) to about $0.35 \text{ g}_{\text{dw}} \text{ cm}^{-3}$ in tolerant genera (Fig. 5.2e). The one outlier is again the understorey tree *Taxus brevifolia* ($0.6 \text{ g}_{\text{dw}} \text{ cm}^{-3}$). Both the mean and variance of wood density was higher in hardwoods than in conifers (Fig. 5.2e,f). Within the intermediate and tolerant classes, hardwood wood densities exceeded those of conifers by a factor of about 1.5. Within the hardwoods, the long-lived pioneers (*Carya* and *Quercus*) had the highest wood densities. It is important to note that shade-tolerance is partly confounded with water availability, as intolerant species tend to occur on drier sites where wood density is often elevated.

In summary, conifers reach higher maximum heights than hardwoods in the intermediate and tolerant classes, and conifers live substantially longer than hardwoods irrespective of shade-tolerance. However, conifers have a lower wood density compared to hardwoods.

5.4 Model Performance and Lessons from the Equilibrium Behaviour

We validated our model against the observed biomass of 41 old-growth stands of known age (see Table 14.3 in Chap. 14 by Lichstein et al., this volume), representing a wide range of forest types and stand ages (60–988 years; median age = 341 years). We assigned each of these 41 validation stands to one of the 106 forest types described above (Sect. 5.2.3). The forest type determined the prescribed species succession for each validation model-run, which was terminated at the actual age of

the validation stand. As in the standard setup (Sect. 5.2.4), we used the mean biomass across 900 patches to characterise the behaviour of the model. Despite the simplicity of the model, and the fact that it ignores edaphic and climatic controls, the model explained 63% of the variation in the old-growth biomass data (Fig. 5.3). This relatively high R^2 suggests that our model should be a useful tool for studying forest carbon stocks. After tuning θ (see Eq. 5.3), the regression line relating observed and predicted values was close to the 1:1 line (Fig. 5.3). Note that this tuning is not species-specific, and therefore has little effect on the R^2 of the validation exercise, but merely ensures that, on average, our model produces reasonable biomass values.

The general behaviour and sensitivity of the model is best understood by examining equilibrium carbon stocks ($C_{x,eq}$) in relation to two key species-specific parameters: maximum height, h_{max} , and longevity, λ (Fig. 5.4). All other parameters in Fig. 5.4, including wood density, were kept constant at the mean conifer or hardwood values.

The biomass equilibrium is controlled mainly by the maximum attainable biomass (which is largely a function of the height-age-curve defined by h_{max}) and the whole-patch mortality rate (which is a function of λ). Within both conifers and hardwoods, $C_{b,eq}$ increases with h_{max} in a slightly concave fashion but with λ in a strongly convex fashion (Fig. 5.4a,b); i.e. the sensitivity of $C_{b,eq}$ to h_{max} is highest for high values of h_{max} , whereas the sensitivity to λ is highest for low values of λ . Our analysis suggests two mechanisms leading to higher $C_{b,eq}$ in coniferous, compared to hardwood, old-growth: (1) Firstly, in North America, conifers occupy higher $C_{b,eq}$ regions of the two-dimensional h_{max} - λ space compared to hardwoods (cf. Figs. 5.4e-f). (2) A second, more subtle, effect is that, for given values of h_{max} and λ , conifers have higher $C_{b,eq}$ than hardwoods due to conifers having higher stand density (which is captured by the volume-height allometries in our model; Fig. 5.1b) and higher biomass expansion factors (Fig. 5.1c). These two factors more

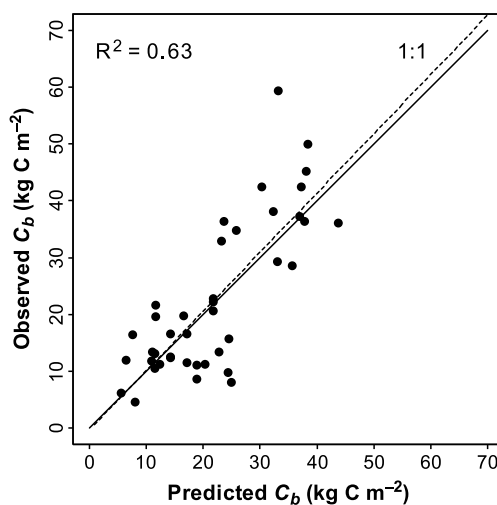


Fig. 5.3 Validation of the model against biomass data from old-growth stands with a known age (see Table 14.3 in Chap. 14 by Lichstein et al., this volume). The 1:1 relationship is shown as a *solid line* and the linear regression between observed and predicted biomasses as a *dashed line* ($C_{b,obs} = -0.34 + 1.04 C_{b,pred}$)

than compensate for the fact that conifers have lower mean wood density than hardwoods.

The equilibrium woody detritus pool, $C_{d,eq}$, is controlled by woody detritus input and the decay rate k_d . Like $C_{b,eq}$, $C_{d,eq}$ increases with h_{max} because tall-statured

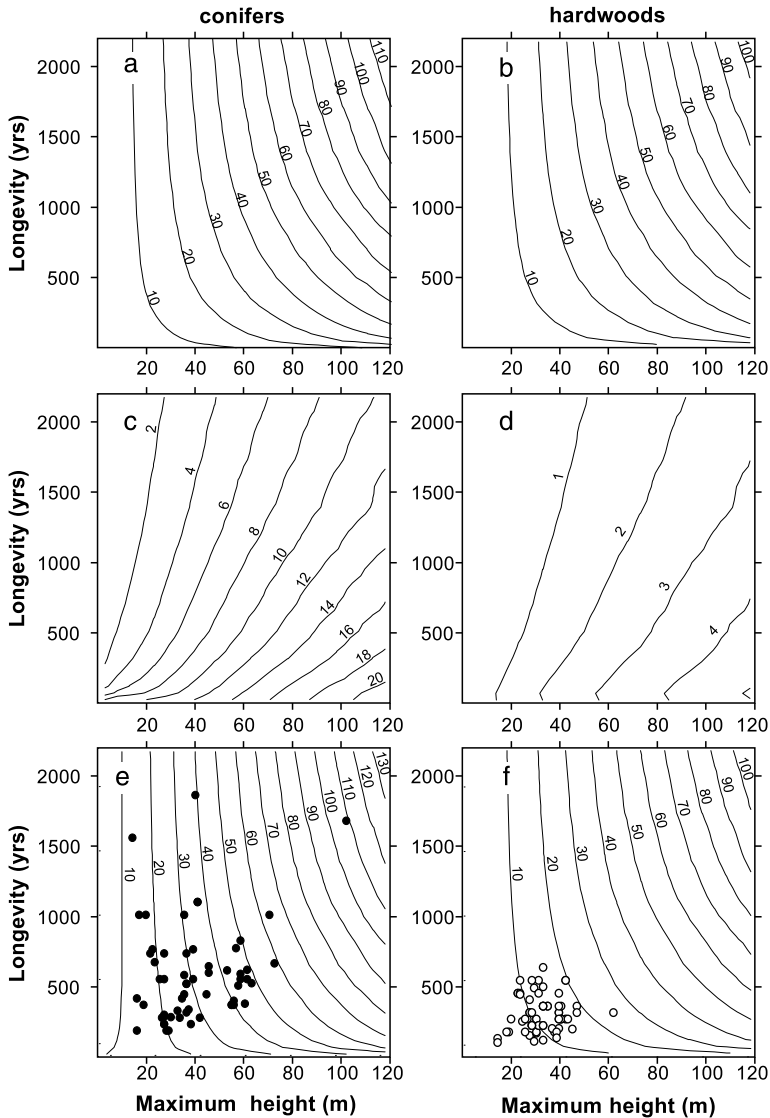


Fig. 5.4 Equilibrium stocks of biomass (a, b), woody detritus (c, d) and total aboveground carbon (e, f) as a function of maximum height (x-axis) and longevity (y-axis) shown separately for coniferous and hardwood monocultures (left and right columns, respectively). Isolines are labelled with carbon stocks in units of kg C m^{-2} . The spectrum of combinations of maximum height and longevity as realised in the tree flora of North America is displayed in panels e and f (filled and open dots, respectively)

forests reach higher biomass levels and therefore – for a given λ – produce more woody detritus (Fig. 5.4c–d). However, unlike $C_{b,eq}$, $C_{d,eq}$ decreases with λ because higher λ implies a lower biomass turnover rate (i.e. slower transfer from biomass to woody detritus). For given values of h_{max} and λ , $C_{d,eq}$ is about four times higher in conifers than in hardwoods (Figs. 5.4c–d) due to the decomposition rates (k_d of 0.03 year⁻¹ in conifers versus 0.1 year⁻¹ in hardwoods).

Total aboveground equilibrium carbon, $C_{a,eq}$, has a similar relationship to h_{max} and λ as $C_{b,eq}$, because $C_{b,eq}$ is much greater in magnitude than $C_{d,eq}$ (Fig. 5.4). However, the difference between conifers and hardwoods (for given values of h_{max} and λ) is greater for $C_{a,eq}$ than for $C_{b,eq}$ due to the additional contribution of $C_{d,eq}$. As with $C_{b,eq}$, conifers advance into regions of higher $C_{a,eq}$ due to their greater size and longevity and due to their steeper equilibrium surface (Fig. 5.4e–f). It is tempting to visualise successional carbon trajectories by moving from one circle (i.e. species) to another across the surfaces in Fig. 5.4. For example, moving from an average hardwood to an average conifer would imply a gain in carbon. Although this equilibrium approach is useful heuristically, it provides only limited insight into successional dynamics because it does not explicitly account for temporal dynamics. Succession, rather than progressing from one equilibrium state to the next, is most likely dominated by transient dynamics. In the next section, we use our model to examine the temporal (i.e. successional) dynamics of carbon stocks.

5.5 The Spectrum of Carbon Trajectories in North American Forests

The spectra of carbon stock changes (ΔC_x) across all 106 FCT during the four successional stages (pioneer, transition, early old-growth, and late old-growth) are shown in Fig. 5.5. Distributions of stock changes during the two earlier stages have substantial spread and are right-skewed. Changes in total aboveground carbon (ΔC_a) during the pioneer stage range from 60 (*Pinus clausa*) to 498 g C m⁻² year⁻¹ (*Sequoia sempervirens*). During the transition phase, the total spread of ΔC_a increases to 340 g C m⁻² year⁻¹, with values ranging from a loss rate of -69 (coastal *Pinus contorta*) to an accumulation rate of 262 g C m⁻² year⁻¹ (transition from *Pinus contorta* to *Pseudotsuga menziesii*). During the early old-growth stage, ΔC_a ranges from carbon losses of -59 g C m⁻² year⁻¹ (*Picea mariana* to *Abies balsamea* in boreal Canada) to a gain of 93 g C m⁻² year⁻¹ (*Pinus monticola* to *Pseudotsuga menziesii*). Absolute values and ranges of biomass change (ΔC_b) were always greater than those of woody detritus (ΔC_d).

Despite the variability, there was a consistent decline in ΔC_a from the pioneer stage to the late old-growth stage (Fig. 5.5). Nevertheless, mean ΔC_a remained positive throughout the first 400 years of succession (126, 58, and 13 g C m⁻² year⁻¹ during the pioneer, transition, and early old-growth stages, respectively), and approached zero only during the late old-growth stage. This

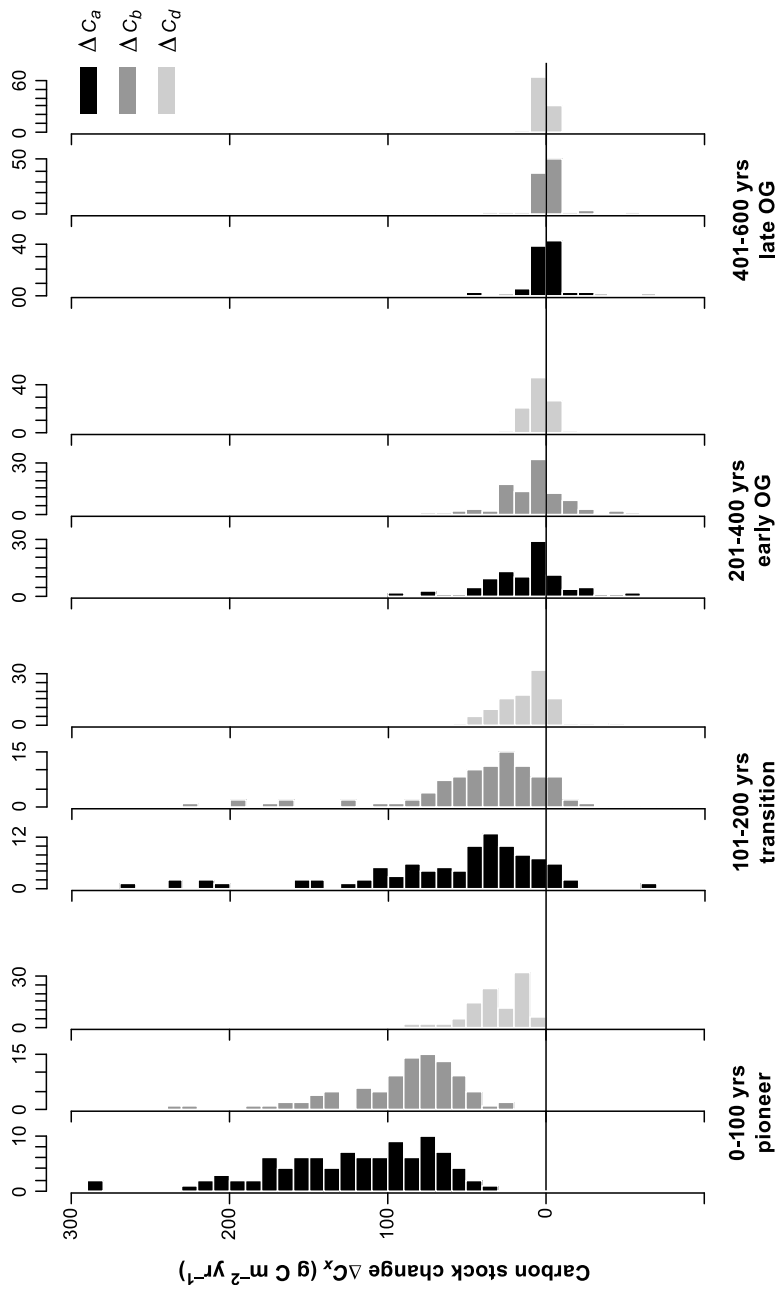


Fig. 5.5 Histograms of aboveground carbon stock changes (ΔC_x) in units of $\text{g C m}^{-2} \text{ year}^{-1}$ for 106 North American forest successions for four successional stages (pioneer: 0–100 years, transition: 101–200 years, early old-growth (OG): 201–400 years and late OG: 401–600 years). The different levels of grey shading indicate the different pools: C_a = Total above-ground carbon (biomass plus woody detritus), C_b = Aboveground biomass carbon, C_d = aboveground woody detritus carbon

result suggests that, on average, shifting traits produce an increase to a late-old-growth asymptote for aboveground carbon stocks in North American forests. Although shifting traits result in late-successional declines in some successions (see below), the results presented here suggest that this is not the typical case. We emphasise that these results represent the effects of shifting traits in isolation of other mechanisms (e.g. synchronised mortality) that may also affect biomass trajectories. The relative contribution of woody detritus to ΔC_a increased over time: From the transition to the early old-growth stage, mean ΔC_b decreased by a factor of 5.5 (from 44 to $8 \text{ g C m}^{-2} \text{ year}^{-1}$), while mean ΔC_d decreased by a factor of 3 (from 12 to $4 \text{ g C m}^{-2} \text{ year}^{-1}$).

5.6 Determinants of Old-Growth Carbon Stock Changes

The previous section examined patterns of aboveground carbon stock changes across the four successional stages. In this section, we focus on the early old-growth stage (201 to 400 years), and ask why certain sequences continue to accumulate carbon while others remain neutral or even lose carbon from the aboveground compartments during this period.

Given that equilibrium carbon stocks were higher in coniferous than in hardwood forests (Fig. 5.4), we might hypothesise that ΔC_a in the carbon balances of old-growth forests is driven by compositional changes that involve transitions between conifers and hardwoods. To test this hypothesis, we classified the 106 successions according to which species groups dominate in the pioneer and late-successional stages. We focus on the seven combinations represented by at least three cover types: (1) conifer to other conifer ($c_i c_j$), (2) conifer to same conifer ($c_i c_i$; i.e. no compositional change), (3) conifer to hardwood (ch), (4) hardwood to conifer (hc), (5) hardwood to other hardwood ($h_i h_j$), (6) mixed conifer-hardwood type to other mixed type ($m_i m_j$), and (7) mixed type to same mixed type ($m_i m_i$).

Substantial carbon accumulation occurred (on average) when conifers were replaced by other conifers ($c_i c_j$). Carbon stock changes were close to zero for all other cases that lacked a shift between conifers and hardwoods ($c_i c_i$, $h_i h_j$, $m_i m_j$, $m_i m_i$). As expected, the change from conifers to hardwoods was associated with carbon losses, while the reverse, a change from hardwoods to conifers, was associated with carbon gains. The above patterns held for total aboveground carbon (ΔC_a ; Fig. 5.6a), biomass (ΔC_b ; Fig. 5.6b), and woody detritus (ΔC_d ; Fig. 5.6d) when group-specific decay rates were used ($k_d = 0.03$ and 0.1 for conifers and hardwoods, respectively). In contrast, ΔC_d was close to zero when the same mean decay rate was used for both conifers and hardwoods (Fig. 5.6c). Thus, accounting for phylogenetic differences in decay rates leads to a predicted loss of woody detritus when conifers (with relatively slow-decomposing detritus) are replaced by hardwoods (with relatively fast-decomposing detritus), and an accumulation of woody detritus when hardwoods are replaced by conifers. The biomass accumulation

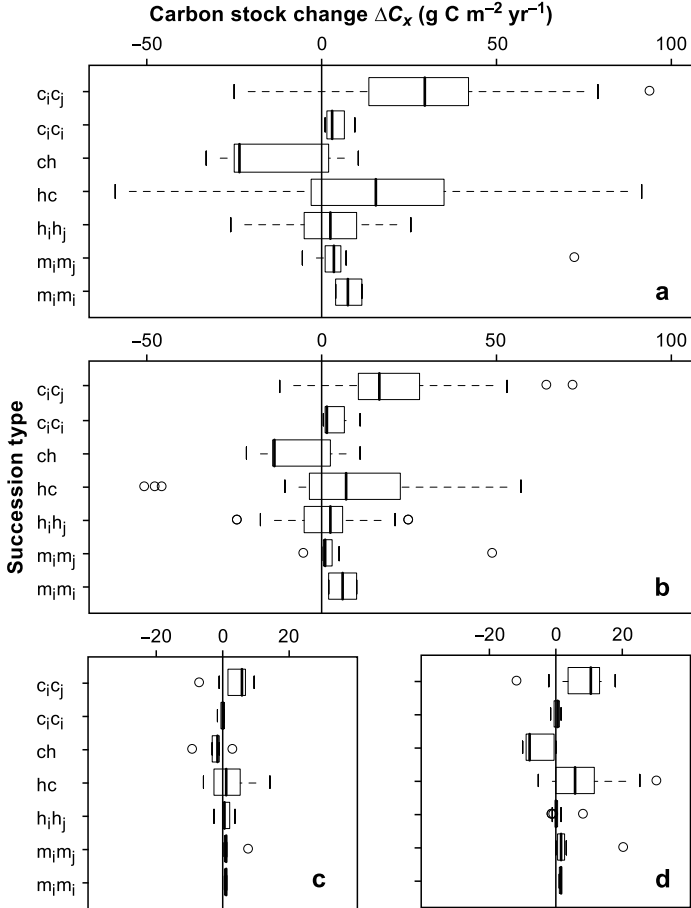


Fig. 5.6 Changes in the total aboveground carbon (a), biomass carbon (b), and wood detritus (c, d) during the early old-growth phase for different types of successional trajectories. In panel c a constant value of k_d of 0.05 year⁻¹ was used for all forest types, and in panel d different values of the decay constant k_d were used for conifers and hardwoods (cf. Table 5.1). The successional trajectories are coded as follows (see also text): *c* dominated by conifers, *h* dominated by hardwoods, *m* mixed. The suffixes *i* and *j* indicate differences in species composition within the three groups. For example, a conifer sequence without species turnover is labelled ‘ $c_i c_i$ ’ whereas one involving species turnover is labelled ‘ $c_i c_j$ ’

effect of changes in species groups is thus amplified by the woody detritus dynamics when phylogenetic differences in decay rates are accounted for. This is partly responsible for the positive correlation between ΔC_b and ΔC_d during the early old-growth stage ($r = 0.70$; Fig. 5.7).

When we compare how changes in the input parameters h_{max} , ρ , and λ between successional stages correlate with carbon stock changes during the early old-growth stage, we see indeed that height differences exhibit the highest degree of correlation

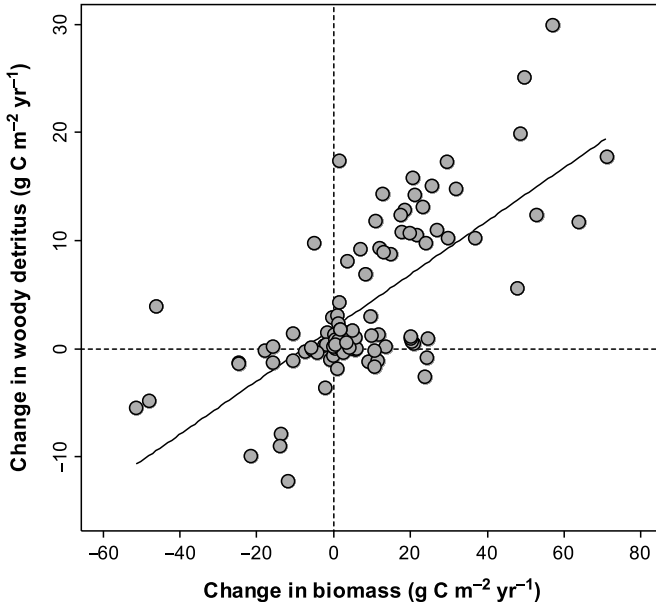


Fig. 5.7 Relationship between changes in biomass and woody detritus carbon stocks during the early old-growth phase in the 106 successions (grey circles) derived from the forest cover type descriptions

Table 5.2 Matrix of Pearson’s correlation coefficients. Carbon stock changes (ΔC_a = total aboveground; ΔC_b = biomass; ΔC_d = woody detritus) refer to the early old-growth stage (201–400 years). Differences in the species-specific parameters h_{max} , ρ , and λ are between the late-successional and the pioneer stages (L–P) and the late-successional and mid-successional stages (L–M)

Δh_{L-M}	$\Delta \rho_{L-P}$	$\Delta \rho_{L-M}$	$\Delta \lambda_{L-P}$	$\Delta \lambda_{L-M}$	ΔC_a	ΔC_b	ΔC_d	
0.429	-0.279	-0.058	-0.004	0.003	0.531	0.515	0.471	Δh_{L-P}
	0.066	0.072	-0.042	0.176	0.354	0.422	0.11	Δh_{L-M}
		0.553	-0.030	0.038	0.060	0.060	0.052	$\Delta \rho_{L-P}$
			0.004	0.141	0.119	0.166	-0.013	$\Delta \rho_{L-M}$
				0.688	-0.017	0.067	-0.239	$\Delta \lambda_{L-P}$
					0.007	0.121	-0.296	$\Delta \lambda_{L-M}$
						0.976	0.835	ΔC_a
							0.698	ΔC_b

($r \sim 0.5$; Table 5.2). The correlation of stock changes with wood density differences is small (between $r = -0.01$ and 0.19) and the correlation of stock changes with longevity differences absent. It is interesting to note that the height difference between late-successionals and pioneers has a higher influence on both ΔC_a and ΔC_b ($r = 0.53$ and 0.51 , respectively) than the difference between late- and mid-successionals ($r = 0.42$ and 0.35 , respectively). Longevity differences seem to

matter only for the changes in woody detritus where an increase in longevity was negatively correlated with ΔC_d .

5.7 Discussion

5.7.1 *Limitations of Our Approach*

Our modelling approach was deliberately simple, and the results are therefore easy to interpret. However, this simplicity is associated with a number of limitations: (1) we considered only two carbon pools – aboveground biomass and woody detritus – and therefore cannot make direct inferences on net ecosystem carbon balance. (2) Because the model considers only carbon, it ignores potential changes in productivity due to shifts in nutrient availability (Pastor and Post 1986; Chap. 9 by Wardle, this volume). (3) Edaphic and climatic effects were not considered when parameterising the model. Thus, the version of the model presented here ignores, for example, intraspecific variation in plant traits due to edaphic or climatic influences. (4) Finally, we prescribed the sequence of species replacement in each forest type based on empirical descriptions. While this is a valid approach for determining the consequences of species turnover, our model obviously cannot be used to study the mechanisms causing the turnover.

The simplicity of our approach arose, in part, from our desire to systematically evaluate the ‘shifting traits’ mechanism across a large geographic area. Thus, the model was centred around a few parameters (h_{\max} , ρ , λ) that were available for most North American tree species and that we suspected a priori to strongly affect carbon dynamics. This simple design allowed us to parameterise the model for the major forest cover types ($n = 106$ successions) and tree species ($n = 182$) of an entire continent. Despite its simplicity, our model explained 63% of the variation in an independent dataset of old-growth forest biomass (see Table 14.3 in Chap. 14 by Lichstein et al., this volume). This suggests that our model captures key features of forest dynamics leading to biomass differences among forest types. Nevertheless, we urge caution in over-interpreting our results for individual successions.

5.7.2 *Comparison with Independent Data*

In the following, we confront our model results with independent data and ask (1) how well we do in predicting the general pattern and magnitude of carbon stock changes with successions – especially during the early old-growth stage –; and (2) to what extent the data provide support for the ‘shifting traits hypothesis’. The data come from three different sources: forest biomass and woody detritus chronosequences (reviewed below), inventories (see Chap. 14 by Lichstein et al., this volume), and an evaluation of a new forest carbon cycle database (see Chap. 15

by Schulze et al., this volume). A more comprehensive synthesis of old-growth carbon dynamics including stock changes inferred from inventories, soil carbon dynamics, and estimates of net ecosystem exchange of CO₂ is provided in the synthesis chapter (Chap. 21 by Wirth).

5.7.2.1 Magnitude of Old-Growth Carbon Stock Changes – Long-Term Chronosequences and Inventories

To our knowledge, there are only 16 aboveground biomass chronosequences for temperate or boreal forests that extend beyond a stand age of 200 years (Fig. 5.8, Table 5.3). Pooling all forest types, the mean (median) biomass changes along these chronosequences during the first four successional stages (pioneer: 0–100 years; transition: 101–200 years; early old-growth: 201–400 years; and late old-growth: 401–600 years) are 91 (75), 32 (20), 19 (12), and 9 (4) g C m⁻² year⁻¹. For the first three stages, this is in good agreement with our model results, where the mean (median) biomass changes were 94 (82), 44 (35), and 8 (5) g C m⁻² year⁻¹ (Fig. 5.9). However, for the later stages, our model predicts lower mean biomass changes than observations would suggest. This is particularly true for the late old-growth stage, where the model suggests equilibrium (–0.2 g C m⁻² year⁻¹) but the data still suggest an increase (see above). The difference between the model and the chronosequences during the early old-growth phase is partly due to the fact that the chronosequences extend to an average age of only 316 years. The modelled biomass change between 201 and 300 years was 12 (8) g C m⁻² year⁻¹, which is closer to the chronosequence estimate. Another important similarity between the model and chronosequences is the predominance of constant or increasing biomass. Except for the Lake Duparquet chronosequence (Paré and Bergeron 1995), no biomass declines were observed in the data.

Of the chronosequences calculated from the US Forest Inventory and Analysis database (FIA; see Chap. 14 by Lichstein et al., this volume) only those from the western US exceeded a time span of 200 years. The FIA data suggest somewhat lower biomass changes during the pioneer and transition stages, but higher rates during the early old-growth stage. However, the high values during the latter are due mostly to the temperate rain forests in the Pacific Northwest.

In addition to the chronosequences summarised above, data on carbon stocks and fluxes in broad stand-age classes were recently compiled for meta-analyses by Pregitzer and Euskirchen (2004) and Schulze et al. (Chap. 15, this volume – based on the database of Luyssaert et al. 2007). In these two studies, the fraction of boreal and temperate forest stands older than 200 years was 9% and 11%, and the fraction of stands older than 400 years only 3% and 2%, respectively. Although the database compiled by Pregitzer and Euskirchen (2004) contains limited biomass data for stands older than 200 years, these are not included in their analysis. Hence, this study is not considered further here. Schulze et al. (Chap. 15, this volume) give an overall mean biomass accumulation rate of 30 g C m⁻² year⁻¹ between stand

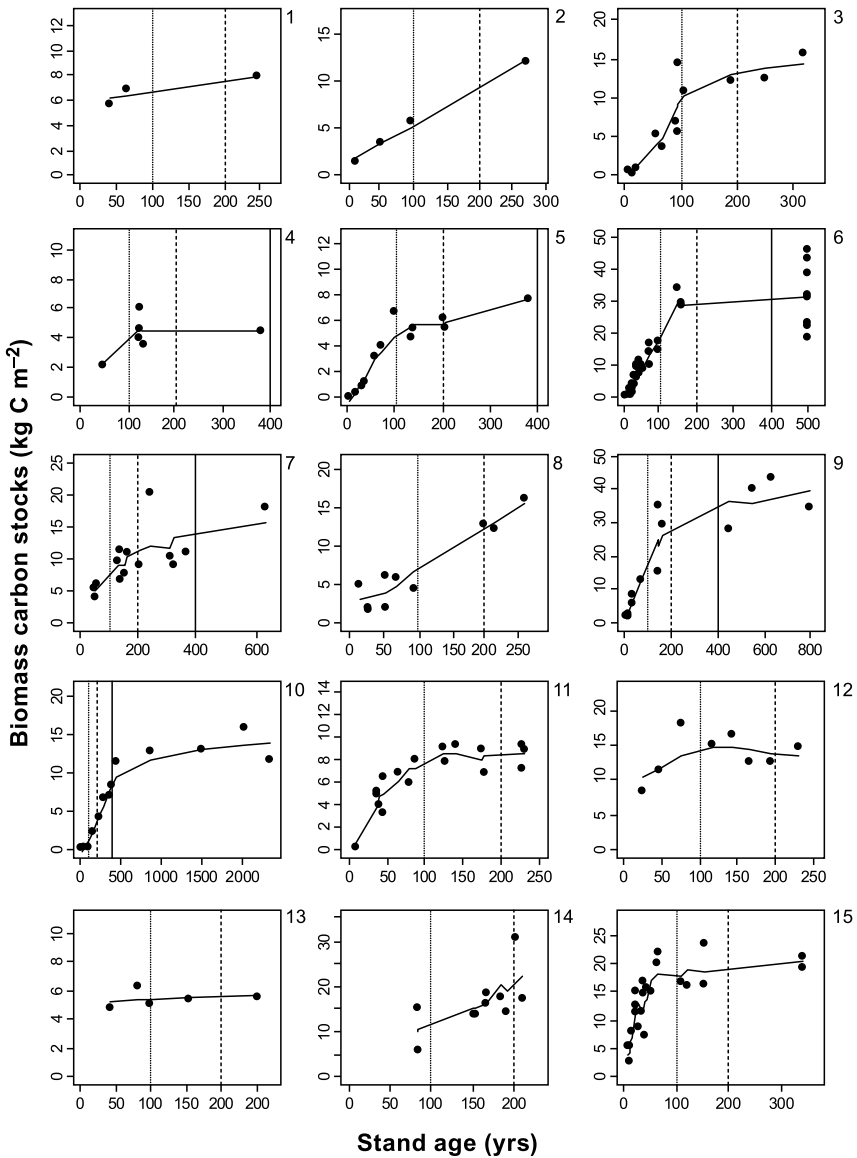


Fig. 5.8: Temperate and boreal chronosequences of aboveground biomass carbon extending to stand ages beyond 200 years. The data (*black dots*) were taken from publications (see legend to Fig. 5.10), and where necessary were digitised from figures. The *vertical lines* delineate the successional stages ‘pioneer,’ ‘transition,’ and ‘early old-growth.’ The intersections between the *vertical lines* and the *fitted curves* were used to calculate the changes in biomass during each successional stage. The curves were fit with Friedman’s super smoother (subsmu-function in R – with parameters *span* = 0.2 and *bass* = 10). The numbers 1–15 indicate the sequences described in Table 5.3

Table 5.3 Temperate and boreal chronosequences of aboveground biomass carbon extending beyond a stand age of 200 years. Labels refer to the panel numbers in Fig. 5.8 (except sequence 16) and to the references listed below the table. For ‘Type’ descriptions, see Sect. 5.6. Species dominating during early and late stages of the succession are listed in the *Pioneer* and *Late* columns, respectively; species abbreviations are given below the table. *P* Pioneer, *T* transition, *EOG* early old-growth $C_{b,x}$ estimated biomass (kg C m^{-2}) at stand age x (years); ΔC_b estimated biomass change ($\text{g C m}^{-2} \text{ year}^{-1}$) in the pioneer (0–100 years), transition (101–200 years), and early old-growth stage (201–400 years)

Label ^a	Name	Type	Duration (years)	Pioneer ^b	Late ^{b,d}	$C_{h,100}$	$C_{h,200}$	$C_{h,400}^*$	ΔC_{b-P}	ΔC_{b-T}	ΔC_{b-EOG}
1	Fraser Exp. Forest	$c_i c_j$	245	Pincon	Pincon	6.4	7.4	8	64	10	13
2	Zotino Pine		270	Pinsyl	Pinsyl	5	9	12.5	50	40	50
3	Metolia		316	Pinpon	Pinpon	10	13	14.3	100	30	11
4	Yakutia		380	Largme	Largme	4	4.5	4.5	40	5	0
5	Zotino lichen Pine		383	Pinsyl	Pinsyl	4.5	6	7.5	45	15	8
6	Wind River Range		500	Psemen	Psemen, Tshet	20	29	31	200	90	10
7	SW Montana		640	Pinalb, Pincon, Piceng ^c , Abilas ^c	Pinalb, Pincon, Piceng ^c , Abilas ^c	8	11	14	80	30	15
8	Cascade Mountains	$c_i c_j$	260	Pinmon, Pincon	Tsumen	7	12	16	70	50	67
9	Andrews		795			16	27	34	160	110	35
10	Michigan Sand Dune		2,348	Pinstr, Pinres ^c	Pinres, Pinstr, Tsucan	2	4	8.5	20	20	23
11	Zotino dark taiga	hc	230	Betsp, Poptre	Abisib, Picobo, Pinsib	7.5	8.1	8.2	75	6	3
12	Lake Duparquet		230	Popbal, Poptre, Betpap	Thuocc, Abibal, Poptre ^c	14	13.5	13.4	140	-5	-3

13	Bonanza Creek		250	Betpap, Poptre	Picgla	5.5	5.7	5.9	55	2	4
14	Adirondack Mountains	mix	410	Betall, Faggra, Picru, Tsucan	Betall, Faggra, Picru, Tsucan	8.0	9.6	14.6	80	16	25
15	Chesapeake Bay	h_i/h_j	340	Lirtul, Quesp.	Faggra, Carsp., Quesp.	17	18	20.5	170	10	18
16	Fontainebleau	h_i/h_i	211	Fagsyl	Fagsyl	10.5	20	20	105	95	-
Mean									91 ± 52	32 ± 36	19 ± 19
Median									75	20	12

^aReferences: 1 Ryan and Waring (1992); 2 Wirth et al. (2002b); 3 Law et al. (2003); 4 Schulze et al. (1995); 5 Wirth et al. (2000b); 6 Jamisch and Harmon (2002); 7 Forcella and Weaver (1977); 8 Boone et al. (1988); 9 Beverly Law, personal communication; 10 Lichter (1998); 11 C. Wirth, unpublished data; 12 Paré and Bergeron (1995); 13, 16 various sources compiled in the Luyssaert et al. (2007) database; 15 Brown and Parker (1994); 16 Keeton et al. (2007)
^bSpecies abbreviations: Abitas *Abies lasiocarpa*, Abisib *Abies sibirica*, Betp *Betula* sp., Betall *Betula alleghaniensis*, Carsp *Carya* sp., Faggra *Fagus grandifolia*, Largme *Larix gemlinii*, Lirtul *Liriodendron tulipiferum*, Piceng *Picea engelmannii*, Picgla *Picea glauca*, Picobo *Picea obovata*, Picrub *Picea rubra*, Pinalb *Pinus albicaulis*, Pincon *Pinus contorta*, Pinmon *Pinus monticola*, Pinpon *Pinus ponderosa*, Pinres *Pinus resinosa*, Pinsib *Pinus sibirica*, Pinstr *Pinus strobus*, Pinsyl *Pinus sylvestris*, Popbal *Populus balsamifera*, Poptre *Populus tremula*, Poptro *Populus tremuloides*, Psemen *Pseudotsuga menziesii*, Quesp *Quercus* sp., Tsucan *Tsuga canadensis*, Tsuhet *Tsuga heterophylla*, Tsumen *Tsuga mertensiana*.
^cSpecies are admixed (i.e. non-dominant).

^dData for the late old-growth stage (LOG: 401–600 years) were available only for four sequences: ΔC_b for the LOG stage are available for sequences 6, 7, 9, and 10 and are 5.1, 8.5, 15.0, and 10.0 g C m⁻² year⁻¹, respectively, with a mean of 9.6 ± 4.1 g C m⁻² year⁻¹

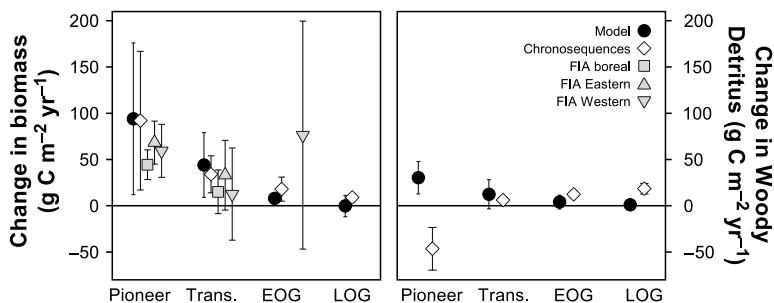


Fig. 5.9 Comparison of modelled and measured changes of aboveground biomass (*left panel*) and coarse woody detritus (*right panel*) in $\text{g C m}^{-2} \text{ year}^{-1}$ within the four successional stages 'pioneer,' *Trans.* 'transition', *EOG* 'early old-growth', and *LOG* 'late old-growth'. *Error bars* standard deviation. The sample unit is a forest sequence. FIA Unites States Forest Inventory and Analysis database (see Chap. 14 by Lichstein et al., this volume)

ages 100 and 300 years, which is in good agreement with the estimates presented above.

In addition, we evaluated the woody detritus chronosequences compiled in Harmon (Table 8.2). As noted by Harmon (Chap. 8), the woody detritus stocks followed either a "reverse J-" or "U-" shaped curve. Mean (median) stock changes during the four successional stages were -46 (-23), 6 (2), 12 (3), and 19 (6) $\text{g C m}^{-2} \text{ year}^{-1}$, respectively. Thus, in contrast to biomass (see above), carbon accumulation rates for woody detritus increased with age. Unlike the woody detritus chronosequences (where young stands may be initiated with a woody detritus 'legacy'), our model considers only de-novo woody detritus (i.e. stands are initiated with zero woody detritus). This explains the large discrepancy between the model prediction and the observation during the pioneer stage (Fig. 5.9). During the succeeding stages all fluxes are positive. The model suggests decreasing accumulation rates 12 (6), 3 (1), and 1 (0.2) $\text{g C m}^{-2} \text{ year}^{-1}$ for the transition, early, and late old-growth stages, respectively, while the observations suggest the opposite (Fig. 5.9 – white diamonds).

These comparisons show that the predictions from our model are roughly in agreement with the few observations we have of biomass accumulation rates in old-growth forests. However, the modelled carbon accumulation in woody detritus is substantially lower than the observed rates, most likely because the latter are based on data from chronosequences from boreal or high-elevation sites with slowly decomposing coniferous woody detritus. For the early old-growth stage, both the data and the model suggest a significant carbon accumulation in the biomass and woody detritus, but the measured rates exceed the modelled rates by factor of 3 (31 versus $11 \text{ g C m}^{-2} \text{ year}^{-1}$) and the discrepancy is even larger for the late old-growth stage (0.8 vs $28 \text{ g C m}^{-2} \text{ year}^{-1}$). We believe that part of the discrepancy is due to the fact that we did not attempt a comparison at the level of FCT (see above). Compared with the spectrum of forest types that we model, in the chronosequence data forest types on marginal sites (boreal, high-elevation, dry) are

over-represented. Trees in such forests tend to grow and decompose more slowly, thus accumulation of carbon is shifted to later stages of stand development compared with forests on more fertile sites. Also, we might have missed an additional mechanism in our model that causes a late-successional carbon accumulation in the biomass and wood detritus.

5.7.2.2 Evidence for the ‘Shifting Traits Hypothesis’

Our model predicts that successional species turnover involving a shift in key traits, particularly h_{\max} , may induce a gain or loss in biomass and woody detritus carbon even late in succession. Given that conifers tend to grow taller than hardwoods, carbon gain is expected if hardwoods are replaced by conifers, and a loss is expected if the reverse happens (Fig. 5.4). However, there are also pronounced differences in stature within the two phylogenetic groups. The available observations for testing the ‘shifting traits hypothesis’ are the 15 true chronosequences in Fig. 5.8 (of which only 10 are from North America) and the six mesic seres extracted from the US inventory data (see Fig. 14.3 in Chap. 14 by Lichstein et al., this volume). For the reasons given in Sect. 5.7.1, we do not attempt a quantitative site-by-site validation of successional trajectories, but rather look at qualitative features.

For the US inventories (Fig. 14.3, op cit.), our model would predict – based on a shift in h_{\max} values – a biomass decline for five successions: the Piedmont transition from *Liriodendron* ($h_{\max} = 61$ m, $\lambda = 250$ years) to *Quercus/Carya* ($h_{\max} \sim 30/33$ m), the New England transition from *Pinus strobus/Quercus rubra* ($h_{\max} = 43/30$ m) to *Quercus/Carya/Acer rubrum* ($h_{\max} = 30/33/28$ m), the Cascade Mountains transition from coastal *Pseudotsuga menziesii* ($h_{\max} = 73$ m) to *Tsuga heterophylla* ($h_{\max} = 52$ m), the Rocky Mountains transition from *Pseudotsuga menziesii* ($h_{\max} \sim 50$ m) to *Picea engelmannii/Abies lasiocarpa* ($h_{\max} = 44/35$ m), and the sub-boreal upper Midwest transition from *Pinus resinosa/Pinus strobus* ($h_{\max} = 32/43$ m) to *Abies balsamea/Picea glauca* ($h_{\max} = 23/55$ m). For four out of these five transitions the inventory data indeed suggest declines, which are, however, small in all but the Cascade Mountains series. No decline occurred in the Rocky Mountain series, most likely because of limited growth rates of *Pseudotsuga* at higher elevation (see legend to Fig. 14.3; Chap. 14 by Lichstein et al., this volume). There are also a number of transitions for which our model would correctly predict a biomass increase, which we do not list individually here.

Only four of the long-term chronosequences in Fig. 5.8 involve pronounced species turnover (panels 8, 11, 12, and 13). The late-successional biomass decline in the Lake Duparquet sequence in panel 12 (Paré and Bergeron et al. 1995) can be explained by a shift in species composition from early-successional hardwoods ($h_{\max} = 23\text{--}27$ m) to shorter, late-successional conifers ($h_{\max} = 22\text{--}23$ m). The relatively constant biomass along the Bonanza Creek sequence in panel 13 is unexpected from the h_{\max} values extracted from the literature for the late-successional *Picea glauca* (55 m) compared to the pioneers *Populus tremuloides*

and *Betula papyrifera* (~ 25 m). However, h_{\max} of *Picea glauca* in the Bonanza Creek LTER does not exceed 30 m (Viereck et al. 1983). This example also illustrates the limitation of our simplistic approach, which ignores site differences in h_{\max} and other parameters. The strong increase in biomass in the Cascade Mountains sequence in panel 8 (Boone et al. 1988) from the early-successional pines, mostly *Pinus contorta* ($h_{\max} = 34$ m), to *Tsuga heterophylla* ($h_{\max} = 52$ m) is expected from the increase in h_{\max} . In the Zotino dark Taiga sequence in panel 11 (C. Wirth, unpublished data), the pioneer phase at around 80 years dominated by *Betula alba* ($h_{\max} = 30$ m) has a biomass that is 2 kg C m^{-2} lower than in the late-successional stage dominated by *Picea obovata* and *Abies sibirica* ($h_{\max} = 40$ m for both species) (Nikolov and Helmisaari 1992). Taken together, these examples illustrate the validity of the ‘shifting traits hypothesis’: knowing the shift in a single trait, h_{\max} , we can confidently predict the direction of change in biomass. The chronosequences in Fig. 5.10 do not allow us to validate our model predictions with respect to woody detritus pools. However, the effect of a change in the decomposition rate with a successional change from hardwoods to conifers is corroborated by the scenario shown in Fig. 8.7c in Chap. 8 by Harmon (this volume), where a change from conifers (slow decay) to hardwoods (fast decay) increased carbon accumulation; the opposite change induced a loss after 200 years.

5.7.3 Why so Few Declines?

While there are successions with a notable decline in biomass, the model results, as well as the chronosequence and inventory data presented in this chapter and in the analysis by Lichstein et al. (Chap. 14), clearly show that declines are the exception rather than the rule.

Citing a lack of appropriate field data to assess successional patterns in forest biomass, Bormann and Likens (1979) used the gap-model JABOWA to predict that New England hardwood forest biomass should peak at around 200 years and then decline towards an asymptote, which is eventually reached after around 350 years (i.e. negative ΔC_b during the early old-growth phase). This led them to postulate the ‘stand-breakup hypothesis’, which provides an elegant argument for late-successional biomass declines and which they believed to have a ‘wide applicability’ in terrestrial ecosystems. Why then is empirical evidence supporting this hypothesis so scarce?

The stand-breakup hypothesis requires a certain degree of synchrony of canopy tree mortality. In the JABOWA model (and many others), there is a hidden synchronisation due to the onset of stress-related mortality when the annual radial increments fall below a threshold, as must occur as the trees approach their maximum diameter (Bugmann 2001). As a consequence, model runs often exhibit damped oscillations of biomass. In our model, some degree of synchronisation among patches occurs as

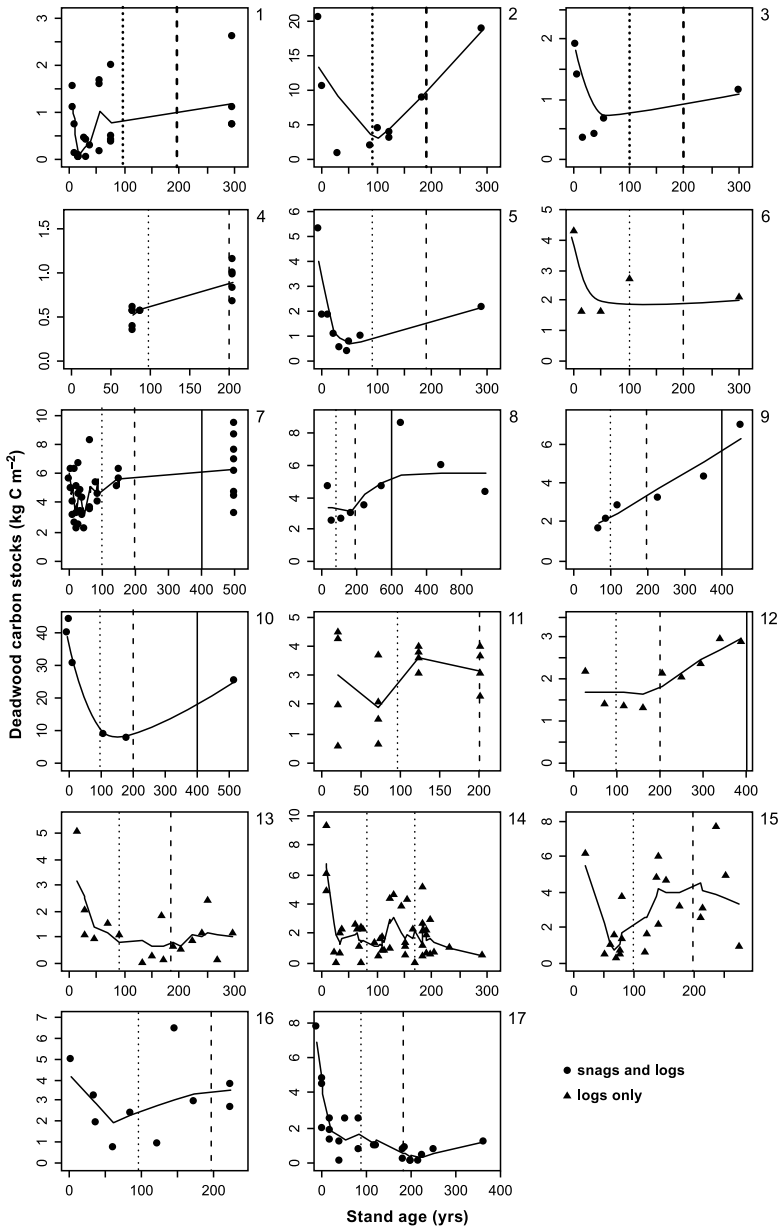


Fig. 5.10 Chronosequences of woody detritus extending to stand ages beyond 200 years. The data were taken from publications listed in Harmon (Chap. 8, Table 8.2, and see below) and where necessary were digitised from figures. Data are the sum of logs and snags (*circles*) or logs only (*triangles*). The chronosequences are arranged in the following order: 1 tropical forests, 2–6 temperate broadleaved, 7–11 temperate needle-leaved, 12–17 boreal needle-leaved. Curves were fit as in Fig. 5.8, except for two sequences with a low number of stands (6 and 10); in these cases,

the whole-patch mortality rate increases simultaneously across patches (Eqs. 5.5, 5.6). The degree of synchronisation is regulated by the parameters δ_1 and δ_2 in Eq. 5.6. Making them higher and more similar to each other increases the degree of synchrony. In the results presented here, we used values of δ_1 and δ_2 that create only a gently synchrony that is not sufficient to induce a pronounced ‘stand breakup’ behavior and subsequent oscillations. Simulations with other values of δ_1 and δ_2 have shown that the ‘shifting traits’ mechanism is still apparent in the biomass trajectories even under extreme synchrony, but the smooth transitions between successional stages become separated by low biomass valleys. Like JABOWA and other gap models, our model is not able to test the stand-break up hypothesis *per se*, because the degree of synchrony is prescribed. Nevertheless, the chronosequences examined in this chapter (Fig. 5.8) and in Chap. 14 suggest that late-successional biomass declines due to stand breakup are rare in temperate and tropical forests.

Several factors may reduce synchrony of mortality in natural forests, thus explaining the scarcity of observed late-successional declines. The pioneer cohort may consist of multiple species that differ in their longevities, so that canopy ‘break up’ would occur over an extended period of time. Alternatively, the pioneer cohort may consist of long-lived pioneers that start to die early on from repeated, small-scale, stochastic disturbances, rather than in a single wave of intrinsically triggered mortality. This happens, for example, in forests characterised by recurring surface fires, where some trees are killed by fire well ahead of their life expectancy, while the surviving trees – released from competition and fertilised by thermal mineralisation – may live even longer than usual (Wirth et al. 2002a).

Peet’s (1981) extension of the stand-breakup hypothesis recognises the importance of the timing of sub-canopy regeneration. If canopy mortality leaves bare gaps (because understorey regeneration is suppressed by the pioneer cohort), then recovery of biomass in these gaps will be delayed until the new recruits attain substantial size. Under continuous regeneration, however, advanced recruits would form a sub-canopy layer with the potential to quickly fill gaps as they are formed. In this case, we would not expect a pronounced biomass decline, because the stand-level mean is not ‘pulled down’ by young patches with low biomass. Continuous regeneration is probably widespread, because most pioneer species – including long-lived pioneers (e.g. species of the genera *Pinus*, *Larix*, *Betula*, *Populus*, *Fraxinus* and some *Quercus* spp.) – have high canopy transparencies, allowing mid- and late-successional species to form dense sub-canopies beneath them

Fig. 5.10 (Continued) the smoothing algorithm failed and curves were drawn by hand. The *vertical lines* delineate the successional stages ‘pioneer,’ ‘transition,’ and ‘early old-growth.’ The intersections between the *vertical lines* and the *fitted curves* were used to calculate the changes in woody detritus during each successional stage. The numbers refer to sequences taken from the following sources: 1 Saldarriaga et al. (1998); 2 Carmona et al. (2001); 3 Roskowski (1980); 4 Shifley et al. (1997); 5 Tritton (1980) (cited in Gore and Patterson 1986); 6 Gore and Patterson (1986); 7 Janisch and Harmon (2002); 8 Spies et al. (1988) (Cascade sequence); 9 Spies et al. (1988) (Coastal sequence); 10 Agee and Huff (1987); 11 Brown and See (1981); 12 Clark et al. (1998); 13-15 Harper et al. (2005) (13 organic, 14 clay, 15 sand); 16 Siberia dark Taiga near Zotino - C. Wirth, unpublished; 17 Wirth et al. (2002b)

(Oliver and Larson 1996). In extreme cases, the understorey regeneration eventually outgrows the still-living pioneers (Schulze et al. 2005), leaving no gap whatsoever.

The ‘shifting trait hypothesis’ suggests yet another mechanism that could prevent a long-term biomass decline due to ‘stand breakup’. A large number of successional pathways exist in which relatively short-statured and short-lived pioneers are replaced by taller and longer-lived late-successional species. With some notable exceptions (see Sect. 5.7.2.2), this is typically the case for conifer-conifer and hardwood-conifer successions. In the few cases where observations suggest a late-successional biomass decline, a shift in traits towards shorter-lived, smaller species may be the underlying driver of the decline rather than ‘stand breakup’ (e.g. Paré and Bergeron 1995; see Fig. 14.3, lowest panel, in Lichstein et al. Chap. 14, this volume).

5.8 Conclusions

Both data and current theories are insufficient to provide a comprehensive picture of old-growth forest carbon dynamics. Beyond a stand age of 200 years, data on forest carbon dynamics are extremely limited. Odum’s ‘equilibrium hypothesis’ and the ‘stand-breakup hypothesis’ by Bormann and Likens (1979) have been the dominant theories predicting either carbon constancy or late-successional declines in carbon stocks as forests age. The latter was largely in line with one prevailing view in forestry management, according to which old stands ‘break up’ and become ‘over-mature’ and ‘senescent’.

The modelling exercise presented in this chapter served three purposes: (1) to integrate available tree trait information and succession descriptions in order to shed new light on late successional carbon trajectories; (2) to provide a systematic account of an alternative theory of forest carbon trajectories, termed the ‘shifting traits hypothesis’; and (3) to characterise and understand the spectrum of carbon fluxes for different phases of stand-development of North American forests. Our main findings are:

- Traits relevant for the build up of biomass and woody detritus carbon stocks (maximum tree height, longevity, and wood density) differ more between phylogenetic groups (conifers vs hardwoods) than between species in different shade-tolerance classes (i.e. successional guilds) within phylogenetic groups. Conifers become taller and are longer-lived than hardwoods. Within conifers, maximum height increased significantly, and wood density decreased significantly, with increasing shade-tolerance.
- Modelled equilibrium biomass increased strongly with increasing maximum height and, to a lesser degree, with increasing longevity. Modelled equilibrium woody detritus also increased with increasing maximum height but decreased with increasing longevity. As a consequence of the opposing effects of longevity on biomass and woody detritus, aboveground carbon stocks were sensitive primarily to maximum height.

- We parameterised the model for 106 North American forest successions, spanning all major forest types on the continent. The model predicts that for most of these successions, 201- to 400-year-old stands (early old-growth) are either carbon-neutral or still accumulating carbon. Few successions exhibited a pronounced late-successional decline. These results are consistent with independent data from inventories and long-term chronosequences. For the late old-growth stage (401–600 years) our model predicts equilibrium behaviour for most successions, when in fact the data suggest continued accumulation of carbon.
- Successions progressing from early- to late-successional conifers, and from early-successional hardwoods to late-successional conifers, tended to accumulate carbon during the early old-growth phase (201–400 years). In the latter case, accumulation was enhanced by the fact that woody detritus of conifers decomposes more slowly than that of hardwoods. In contrast, successions progressing from early-successional conifers to late-successional hardwoods tended to lose carbon during the early old-growth stage.
- In trying to understand why late successional declines in aboveground carbon stocks are so rare (both in our model predictions and empirical data), we explored a range of explanations. The ‘shifting trait hypothesis’, where trait combinations change along succession predominantly from short/short-lived to tall/long-lived species, is only one of them. A lack of synchronous canopy mortality and a buffering effect of understorey regeneration may additionally operate to prevent late-successional declines.

Acknowledgements We would like to thank Hans Dähring for setting up the model runs and members of the FET database team (Dorothea Frank, Steffi Nöllert, Gerhard Bönisch, Jens Kattge, Kiona Ogle, and Anja Fankhänel) for invaluable help with parameter acquisition. We are also indebted to Thomas Wutzler for providing the yield table database and to Beverly Law for allowing us to present her unpublished biomass data of the Andrews chronosequence in Fig. 5.8, panel 9.

References

- Agee JK, Huff MH (1987) Fuel succession in a western hemlock/Douglas-fir forest. *Can J For Res* 17(7):697–704
- Assmann E (1961) *Waldertragskunde*. BLV, München
- Assmann E, Franz F (1965) Vorläufige Fichten-Ertragstafel für Bayern. *Forstw Cbl* 84
- Badeck F-W, Lischke H, Bugmann H, Hickler T, Hönninger K, Lasch P, Lexer MJ, Mouillot F, Schaber J, Smith B (2001) Tree species composition in European pristine forests: comparison of stand data to model predictions. *Climatic Change* 51:307–347
- Bazzaz FA (1979) The physiological ecology of plant succession. *Annu Rev Ecol Systematics* 10:351–371
- Boone RD, Sollins P, Cromack K Jr (1988) Stand and soil changes along a mountain hemlock death and regrowth sequence. *Ecology* 69:714–722
- Bormann FH, Likens GE (1979) *Pattern and process in a forested ecosystem*. Springer, New York

- Botkin DB (1981) Causality and succession. In: West DC, Shugart HH, Botkin DB (eds) *Forest succession: concepts and application*. Springer, New York, pp 36–55
- Brown JK, See TE (1981) Downed dead woody fuel and biomass in the northern Rocky Mountains. U.S. Department of Agriculture, Forest Service, Intermountain Forest and Range Experiment Station, General Technical Report INT-117, pp 48
- Brown MJ, Parker GG (1994) Canopy light transmittance in a chronosequence of mixed-species deciduous forests. *Can J For Res* 24:1694–1703
- Bugmann H (2001) A review of forest gap models. *Climatic Change* 51:259–305
- Burns RM, Honkala BH (1990) *Silvics of North America: 1. Conifers; 2. Hardwoods*. Agriculture Handbook 654. United States Department of Agriculture, Forest Service, Washington, DC
- Carmona MR, Armesto JJ, Aravena JC, Pérez CA (2002) Coarse woody detritus biomass in successional and primary temperate forests in Chiloé Island, Chile. *For Ecol Manage* 164:265–275
- Clark DF, Kneeshaw DD, Burton PJ, Antos JA (1998) Coarse woody debris in sub-boreal spruce forests of west-central British Columbia. *Can J For Res* 28:284–290
- Dittmar O, Knapp E, Lembcke G (1986) DDR Buchenertragstafel 1983
- Doyle TW (1981) The role of disturbance in the gap dynamics of a montane rain forest: an application of a tropical forest succession model. In: West DC, Shugart HH, Botkin DB (eds) *Forest succession: concepts and application*. Springer, New York, pp 56–73
- Erteld W (1962) Wachstumsgang und Vorratsbehandlung der Eiche im norddeutschen Diluvium 11:1155–1176
- Eyre FH (ed) (1980) *Forest cover types of the United States and Canada*. Society of American Foresters, Washington, DC, p 148
- Forcella F, Weaver T (1977) Biomass and productivity of subalpine *Pinus albicaulis* – *vaccinium scoparium* association in Montana, USA. *Vegetatio* 35:95–105
- Franklin JF, Hemstrom MA (1981) Aspects of succession in the coniferous forests of the Pacific Northwest. In: West DC, Shugart HH, Botkin DB (eds) *Forest succession: concepts and application*. Springer, New York, pp 212–229
- Glenn-Lewin DC, Peet RK, Veblen TT (1992) *Plant succession – theory and prediction*. Chapman and Hall, London
- Gore JA, Patterson WA III (1986) Mass of downed wood in northern hardwood forests in New Hampshire: potential effects of forest management. *Can J For Res* 16:335–339
- Harper KA, Bergeron Y, Drapeau P, Gauthier S, De Grandpré L (2005) Structural development following fire in black spruce boreal forest. *For Ecol Manage* 206:293–306
- Henry HAL, Aarssen LW (2001) Inter- and intraspecific relationships between shade tolerance and shade avoidance in temperate trees. *Oikos* 93:477–487
- Hickler T, Smith B, Sykes MT, Davis MB, Sugita S, Walker K (2004) Using a generalized vegetation model to simulate vegetation dynamics in northeastern USA. *Ecology* 85:519–530
- Horn HS (1974) The ecology of secondary succession. *Annu Rev Ecol Syst* 5:25–37
- Horn HS (1981) Some causes of variety in patterns of secondary succession. In: West DC, Shugart HH, Botkin DB (eds) *Forest succession: concepts and application*. Springer, New York, pp 24–35
- Hubbel SP (2001) *The unified neutral theory of biodiversity and biogeography*. Princeton University Press, Princeton, NJ
- Janisch JE, Harmon ME (2002) Successional changes in live and dead wood carbon stores: implications for net ecosystem productivity. *Tree Physiol* 22:77–89
- Jenkins JC, Chojnacky DC, Heath LS, Birdsey RA (2004) Comprehensive database of diameter-based biomass regressions for North American tree species. General Technical Report NE-319, USDA Forest Service, Northeastern Research Station, Newtown Square, PA, pp 1–45
- Kattge J, Wirth C, Nöllert S, Bönisch G (2008) Functional Ecology of Trees database (<http://www.bgc-jena.mpg.de/bgc-organisms/pmwiki.php/Research/FET>)
- Keeton WS, Kraft CE, Warren DR (2007) Mature and old-growth riparian forests: structure, dynamics, and effects on adirondack stream habitats. *Ecol Appl* 17:852–868

- Kobe RK, Pacala SW, Silander JA Jr, Canham CD (1995) Juvenile tree survivorship as a component of shade tolerance. *Ecol Appl* 5:517–532
- Körner C (2005) An introduction to the functional diversity of temperate forest trees. In: Scherer-Lorenzen M, Körner C, Schulze E-D (eds) *Forest diversity and function: temperate and boreal systems*. Springer, Berlin, pp 13–37
- Law BE, Sun OJ, Campbell J, Van Tuyl S, Thornton PE (2003) Changes in carbon storage and fluxes in a chronosequence of ponderosa pine. *Glob Change Biol* 9:510–524
- Lichter J (1998) Primary succession and forest development on coastal Lake Michigan sand dunes. *Ecol Monogr* 68:487–510
- Lusk CH, Contreras O (1999) Foliage area and crown nitrogen turnover in temperate rain forest juvenile trees of differing shade tolerance. *J Ecol* 87:973–983
- Luyssaert S, Inglisma I, Jung M, Richardson AD, Reichstein M, Papale D, Piao SL, Schulze ED, Wingate L, Matteucci G, Aragao L, Aubinet M, Beers C, Bernhofer C, Black KG, Bonal D, Bonnefond J-M, Chambers J, Ciais P, Cook B, Davis KJ, Dolman AJ, Gielen B, Goulden M, Grace J, Granier A, Grelle A, Griffis T, Grünwald T, Guidolotti G, Hanson PJ, Harding R, Hollinger DY, Hutryra LR, Kolari P, Kruijt B, Kutsch W, Lagergren F, Laurila T, Law BE, Le Maire G, Lindroth A, Loustau D, Malhi Y, Mateus J, Migliavacca M, Misson L, Montagnani L, Moncrieff J, Moors E, Munger JW, Nikinmaa E, Ollinger SV, Pita G, Rebmann C, Rouspard O, Saigusa N, Sanz MJ, Seufert G, Sierra C, Smith M-L, Tang J, Valentini R, Vesala T, Janssens IA (2007) CO₂ balance of boreal, temperate, and tropical forests derived from a global database. *Glob Change Biol* 13:2509–2537
- McArdle RE (1961) The yield of Douglas fir in the Pacific Northwest. In: *USDA Tech Bull 201* Washington, DC, p 74
- Niinemets U, Valladares F (2006) Tolerance to shade, drought, and waterlogging of temperate Northern Hemisphere trees and shrubs. *Ecol Monogr* 76:521–547
- Nikolov N, Helmisaari H (1992) Silvics of the circumpolar boreal forest species. In: Shugart HH, Leemans R, Bonan GB (eds) *A systems analysis of the global boreal forest*. Cambridge University Press, Cambridge, p 565
- Odum EP (1969) Strategy of ecosystem development. *Science* 164:262–270
- Oliver CD, Larson BC (1996) *Forest stand dynamics, update edn*. Wiley, New York
- Olsen JS (1981) Carbon balance in relation to fire regimes. In: *Proceedings of the Conference Fire regimes and ecosystem properties*. USDA Forest Service, Honolulu, pp 327–378
- Pacala SW, Canham CD, Silander JA, Kobe RK (1994) Sapling growth as a function of resources in a north temperate forest. *Can J For Res-Rev Can Rech For* 24, 2172–2183
- Pacala SW, Canham CD, Saponara J, Silander JA Jr, Kobe RK, Ribbens E (1996) Forest models defined by field measurements: estimation, error analysis and dynamics. *Ecol Monogr* 66:1–43
- Paré D, Bergeron Y (1995) Above-ground biomass accumulation along a 230-year chronosequence in the southern portion of the Canadian boreal forest. *J Ecol* 83:1001–1007
- Pastor J, Post WM (1986) Influence of climate, soil-moisture, and succession on forest carbon and nitrogen cycles. *Biogeochemistry* 2:3–27
- Peet RK (1981) Changes in biomass and production during secondary forest succession. In: West DC, Shugart HH, Botkin DB (eds) *Forest succession: concepts and application*. Springer, New York, pp 324–338
- Peet RK (1992) Community structure and ecosystem function. In: Glenn-Lewin DC, Peet RK, Veblen TT (eds) *Plant succession: theory and prediction*, Chapman and Hall, London, pp 103–151
- Pregitzer KS, Euskirchen ES (2004) Carbon cycling and storage in world forests: biome patterns related to forest age. *Glob Change Biol* 10:2052–2077
- Purves DW, Lichstein JW, Strigun N, Pacala SW (2008) Predicting and understanding forest dynamics using a simple, tractable model. *Proc Natl Acad Sci USA* 105:17018–17022
- Roskowski JP (1980) Nitrogen fixation in hardwood forests of the northeastern United States. *Plant Soil* 54:33–44

- Ryan MG, Waring RH (1992) Maintenance respiration and stand development in a subalpine lodgepole pine forest. *Ecology* 73:2100–2108
- Saldarriaga JG, West DC, Tharp ML, Uhl C (1988) Long-term chronosequence of forest succession in the upper Rio Negro of Colombia and Venezuela. *J Ecol* 76:939–958
- Schulze ED, Schulze W, Kelliher FM, Vygodskaya NN, Ziegler W, Kobak KI, Koch H, Arneth A, Kusnetsova WA, Sogatchev A, Issajev A, Bauer G, Hollinger DY (1995) Aboveground biomass and nitrogen nutrition in a chronosequence of pristine dahurian larch stands in eastern Siberia. *Can J For Res-Rev Can Rech For* 25:943–960
- Schulze ED, Wirth C, Mollicone D, Ziegler W (2005) Succession after stand replacing disturbances by fire, wind throw, and insects in the dark Taiga of Central Siberia. *Oecologia* 146:77–88
- Shifley SR, Brookshire BL, Larsen DR, Herbeck LA (1997) Snags and down wood in Missouri old-growth and mature second-growth forests. *North J Appl For* 14(4):165–172
- Shugart HH (1984) A theory of forest dynamics. The ecological implications of forest succession models. Springer, New York
- Shugart HH, Smith TM (1996) A review of forest patch models and their application to global change research. *Climatic Change* 34:131–153
- Shugart HH, West DC (1981) Long-term dynamics of forest ecosystems. *Am Sci* 69:647–652
- Spies TA, Franklin JF, Thomas TB (1988) Coarse woody debris in Douglas-fir forests of western Oregon and Washington. *Ecology* 69:1689–1702
- Tjurin A, Naumenko I (1956) Forstliches Hilfsbuch für Waldtaxation, Moskva
- Urban DL, Bonan GB, Smith TM, Shugart HH (1991) Spatial applications of gap models. *For Ecol Manage* 42:95–110
- Viereck LA, Dyrness CT, Van Cleve K, Foote MJ (1983) Vegetation, soils, and forest productivity in selected forest types in interior Alaska. *Can J For Res* 13:703–720
- Walters MB, Reich PB (1999) Low-light carbon balance and shade tolerance in the seedlings of woody plants: do winter deciduous and broad-leaved evergreen species differ? *New Phytol* 143:143–154
- Watt AS (1947) Pattern and process in the plant community. *J Ecol* 35:1–22
- Wenk G, Römisch G, Gerold D (1985) DDR-Fichtenertragstafel 1984. Agrarwissenschaftliche Gesellschaft der DDR, Technische Universität Dresden - Sektion Forstwissenschaft
- West DC, Shugart HH, Botkin DB (1981) Forest succession - concepts and application. Springer, New York
- Wimmenauer (1919) Wachstum und Ertrag der Esche. *Allg Forst- Jagdz* 95:2–17
- Wirth C, Czimczik CI, Schulze E-D (2002a) Beyond annual budgets: carbon flux at different temporal scales in fire-prone Siberian Scots pine forests. *Tellus Ser B Chem Phys Meteorol* 54:611–630
- Wirth C, Schulze E-D, Lühker B, Grigoriev S, Siry M, Harges G, Ziegler W, Backor M, Bauer G, Vygodskaya NN (2002b) Fire and site type effects on the long-term carbon and nitrogen balance in pristine Siberian Scots pine forests. *Plant Soil* 242:41–63
- Wirth C, Schulze E-D, Schwalbe C, Tomczyk S, Weber G, Weller E (2004a) Dynamik der Kohlenstoffvorräte in den Wäldern Thüringens – Modelluntersuchung zur Umsetzung des Kyoto-Protokolls. Thüringer Landesanstalt für Wald, Jagd und Fischerei, Gotha
- Wirth C, Schumacher J, Schulze E-D (2004b) Generic biomass functions for Norway spruce in Central Europe – a meta-analysis approach towards prediction and uncertainty estimation. *Tree Physiol* 24:121–139
- Wright SJ, Muller-Landau HC, Condit R, Hubbell SP (2003) Gap-dependent recruitment, realized vital rates, and size distributions of tropical trees. *Ecology* 84:3174–3185